

Basalt Fiber Sheets for shear Strengthening of Deep Beams with Openings

^a Hala Mamdouh, ^b Hoda A. Awad, ^c Mostafa A. Osman

^a Associate Professor, Civil Engineering Department, Faculty of Engineering at Mataria, Helwan University, Cairo 11718, Egypt.

^b Ph.D. Student, Civil Engineering Department, Faculty of Engineering at Mataria, Helwan University, Cairo 11718,

^c Professor, Civil Engineering Department, Faculty of Engineering at Mataria, Helwan University, Cairo 11718, Egypt.

DOI: <https://doi.org/10.5281/zenodo.11635043>

Published Date: 13-June-2024

Abstract: Research into reinforcing reinforced concrete (RC) deep beams with apertures using externally bonded basalt fiber reinforced polymer (BFRP) composite sheets is detailed in this article.

Nine deep beams with holes were built and put through their paces with a three-point load. A total length of 1000 mm and a cross-section of 150 x 500 mm were the dimensions of the test specimen. At the beam's midpoint, two holes were symmetrically positioned; one hole was in each shear span. Opening shapes and BFRP sheet orientation were among the test factors.

The degree to which the normal load route was interrupted largely determined the structural response of RC deep beams with apertures. The shear strength of RC deep beams was enhanced more by horizontally bonded BFRP strengthening around the apertures than by vertical strengthening.

The horizontal BFRP sheets increased the material's strength by 8–54%. Whereas, between zero and eighteen percent, strength is increased by means of vertical BFRP. An analytical technique was presented and compared with test results for the prediction of shear strength in RC deep beams with apertures reinforced with BFRP sheets.

Keywords: Basalt fiber -reinforced polymer (BFRP) sheets, Deep beams, Openings, Strengthening, horizontally, vertically.

1. INTRODUCTION

In tall buildings, deep beams can resist high loads on structures, such as girders, shear walls, caissons, pile caps, wall footings, diaphragms, and complex foundation systems. **de Paiva(1965)**, **Ramakrishnan and Ananthanarayana, (1968)**, **Arabzadeh (2001)**. Openings are necessary for accessibility and to provide air, power, and network services, however they reduce deep beam strength, fracture, and deflect.

Additionally, openings disturb normal stress flow, concentrating tension at the apertures' edges and causing concrete breaking early. **Campione, and Minafò. (2012)**. Therefore many researchers studied the parameters that affect the presence of openings in deep beams (location and dimensions of openings) to know the problems caused by these openings, **Hwang et al (2000)**, **Karimizadeh and Arabzadeh (2021)** studied the behavior of deep beams with openings having rectangular sections. **Ata El-Kareim et al (2020)** cared with T-shaped sections as they studied experimentally the behavior of flanged deep beams with web openings while **Ghali MK et al (2021)** studied numerically the Behavior of T-shaped deep beams with openings using different loading conditions.

In parallel to that, many researchers have been trying to solve the problems that the opening cause in deep beams by strengthening them with FRP composites, especially by using carbon fibers. **El Maaddawy T and Sherif S (2009)** investigated the shear strength of 13 deep beams with openings using CFRP composites testing it under four points and they achieved that the existence of CFRP around the opening increases the shear strength in the range from 35-73%. while, **Hawileh RA et al (2012)** used non-linear analysis to study the effect of CFRP in strengthening openings in deep beams. Then **WY Lu et al (2015)** tested 18 H.S.C deep beams with web openings strengthened with CFRP, 6 beams were strengthened horizontally and 6 are strengthened vertically with 4 layers of CFRP they reached the horizontal CFRP increasing the shear strength by 6% while the vertical increase the strength by 10%. After that **Rahim NI et al (2020)** tested 9 deep beams with openings strengthened with carbon fiber and 1 control deep beam without opening under four-point loads, they achieved that the capacity was increased by about 10-40 % and the most effective number of layers is 2 and 3 layers for sizes 150 and 200 mm respectively. **Khalaf, M.et al (2021)** tested 3 externally strengthened continuous deep beams with large openings under 5 points load they achieved that the CFRP enhances the strength by 17 %. **Karimizadeh H et al (2022)** tested 11 deep beams with square openings strengthened with CFRP using two techniques (externally bonded and externally bonded with grooves) and steel protective frames (SPF) applied to 3-point loads, the results showed that the capacity increased by 42%,58%, and 115% when using those techniques respectively. however, some researchers turned to strengthen openings using other fibers such as, **Qudeer Hussain and Amorn Pimanmas (2015)** who tested 29 deep beams with web openings using 3-point loads and strengthen the opening by sprayed GFRP and they concluded that GFRP is more effective in normal strength concrete than that in high strength concrete, the author chose this fiber as it has mechanical properties better than that of glass fiber and its cost is lower than that of carbon fiber. Also, basalt fiber (BF) is easy to handle and process, so there is no need for special processing equipment, it can be recycled and is environmentally friendly and it is convenient with a lot of resins like epoxy, it has excellent shock resistance as it is good for ballistic applications **Ramakrishnan and Panchalan (2005)** ,**Shetty and Jain (2019)**.

Externally bonded BFRP sheets have not been shown to increase the shear capacity of apertured RC deep beams. Shear strength estimate for RC deep beams with BFRP-sheeted apertures is undefined. This structural engineering method is then examined to improve RC deep beams with different apertures. Experimental data will enable engineers and researchers understand how BFRP sheets affect the opening presence, shapes, strength, and failure mechanism of RC deep beams. Literature data was used to forecast shear strength of BFRP shear-strengthened RC deep beams with apertures and compare test results.

2. EXPERIMENTAL PROGRAM

The experimental program consists of nine deep beams divided into four groups listed in Table (1). Group 1 consists of three deep beams with vertical rectangle openings with dimensions 100*200 mm, group 2 consists of 2 deep beams with horizontal rectangle openings with dimensions 200*100 mm, Group 3 consists of two deep beams with circle openings with 160 mm diameter and Group 4 consists of two deep beams with square openings having a length of 140 mm. Figure (2) illustrates the positions and size of apertures in all specimens, which have the same cross-section with 150 mm, 500 mm, and 1000 mm diameters and 850 mm clear spans. Figure (3) illustrates the beam span and concrete cross-section.

Table (1): The experimental program

Group no.	Beam symbol*	Type of opening	Direction of opening	Size of opening(mm)	Fiber direction
G1	NS-VRO	Rectangular	Vertical	100 *200	-
	VS-VRO	Rectangular	Vertical	100 *200	Vertical
	HS-VRO	Rectangular	Vertical	100 *200	Horizontal
G2	VS-HRO	Rectangular	Horizontal	200 *100	Vertical
	HS-HRO	Rectangular	Horizontal	200 *100	Horizontal
G3	VS-CO	Circular	-	D=160	Vertical
	HS-CO	Circular	-	D=160	Horizontal
G4	VS-SO	Square	-	140 *140	Vertical
	HS-SO	Square	-	140 *140	Horizontal

*NS, VS, and HS refer to no strengthening, vertical strengthening, and horizontal strengthening respectively. RO, HRO, CO, and SO refer to vertical rectangle opening, horizontal rectangle opening, circular opening, and square opening respectively.

2.1 Material properties

Beams were cast utilizing local resources, including Portland cement, siliceous sand, and excellent dolomite with a maximum nominal size of 20 mm. and the steel used for stirrups is mild steel with $(F_y)=240$ MPa with 6 mm diameter bars and high-tensile steel for longitudinal bars with $(F_y)=360$ MPa with 25 mm diameter at the top and have a rough surface to get more bonds between steel bars and concrete. The bottom reinforcement of beams was 2 bars with 16mm, Clean drinking water is used in this work. BFRP sheets with a thickness of 0.36 mm are used, 3 specimens of BFRP sheets are roughed with sand and tested to get stress-strain curve for the sheet (figure1) and the used resin is epoxy of type Sikadur – 330. The properties of BF laminate and epoxy used are shown in Table (2)

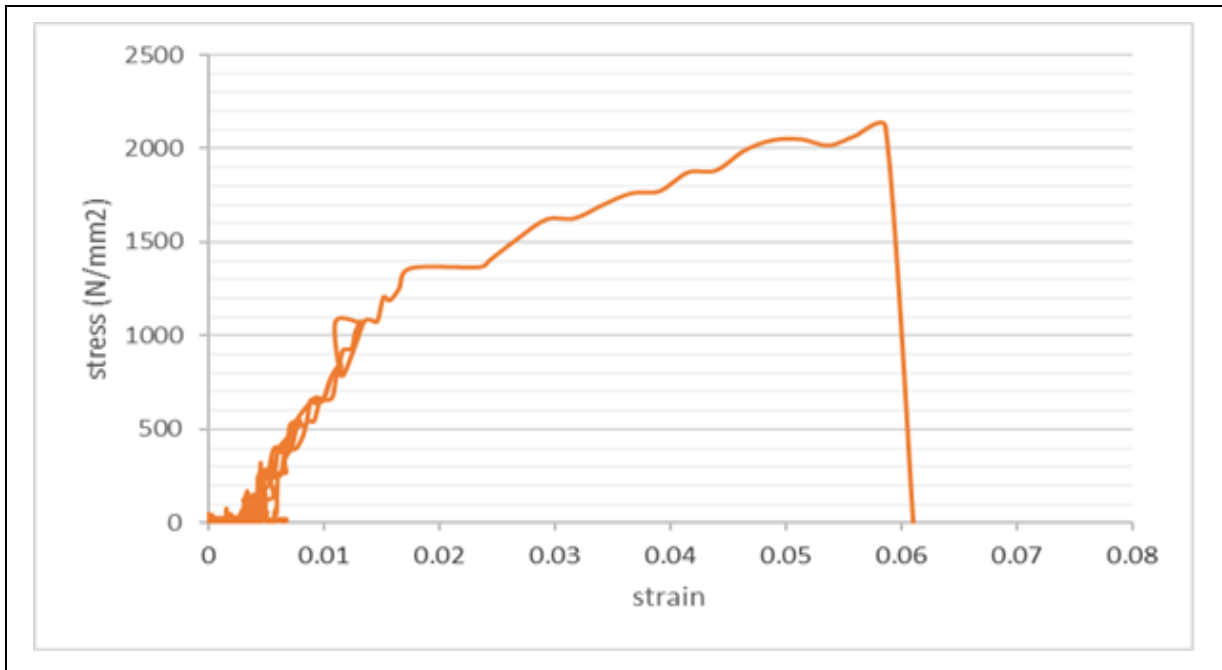


Figure (1) : stress-stain curve for basalt sheets

Table (2): The properties of different types of materials (BF sheets and epoxy)

Material	Basalt fiber sheets	Epoxy
Type	BWUD-400	Sikadur-330
Tensile Strength (MPa)	2148.19	30
Elongation at Failure (%)	2.5	-
Tensile Modulus (MPa)	50.5	3.8
Fabric Density (g/m ²)	400	-
Mixing Ratio by Weight	-	A: B, 4: 1

2.2 Strengthening system of beams

Fig. 4, represents a schematic of the BFRP plan employed for external shear strengthening is presented. To successfully increase the beam's shear strength, the BFRP sheets must be able to block any possible shear cracks. Two layers of longitudinal BFRP sheets with a 100 mm x 1000 mm size and fibers orientated parallel to the longitudinal axis of the beam were glued to the concrete above and below each opening. Additionally, two layers of BFRP sheets with fibers orientated vertically were wrapped behind the chords on the right and left for each opening with a size of 100 mm and a length of 500 mm, and they were placed next to each vertical face of the openings with fibres oriented vertically for each opening with a size of 100 mm and a length of 500 mm.

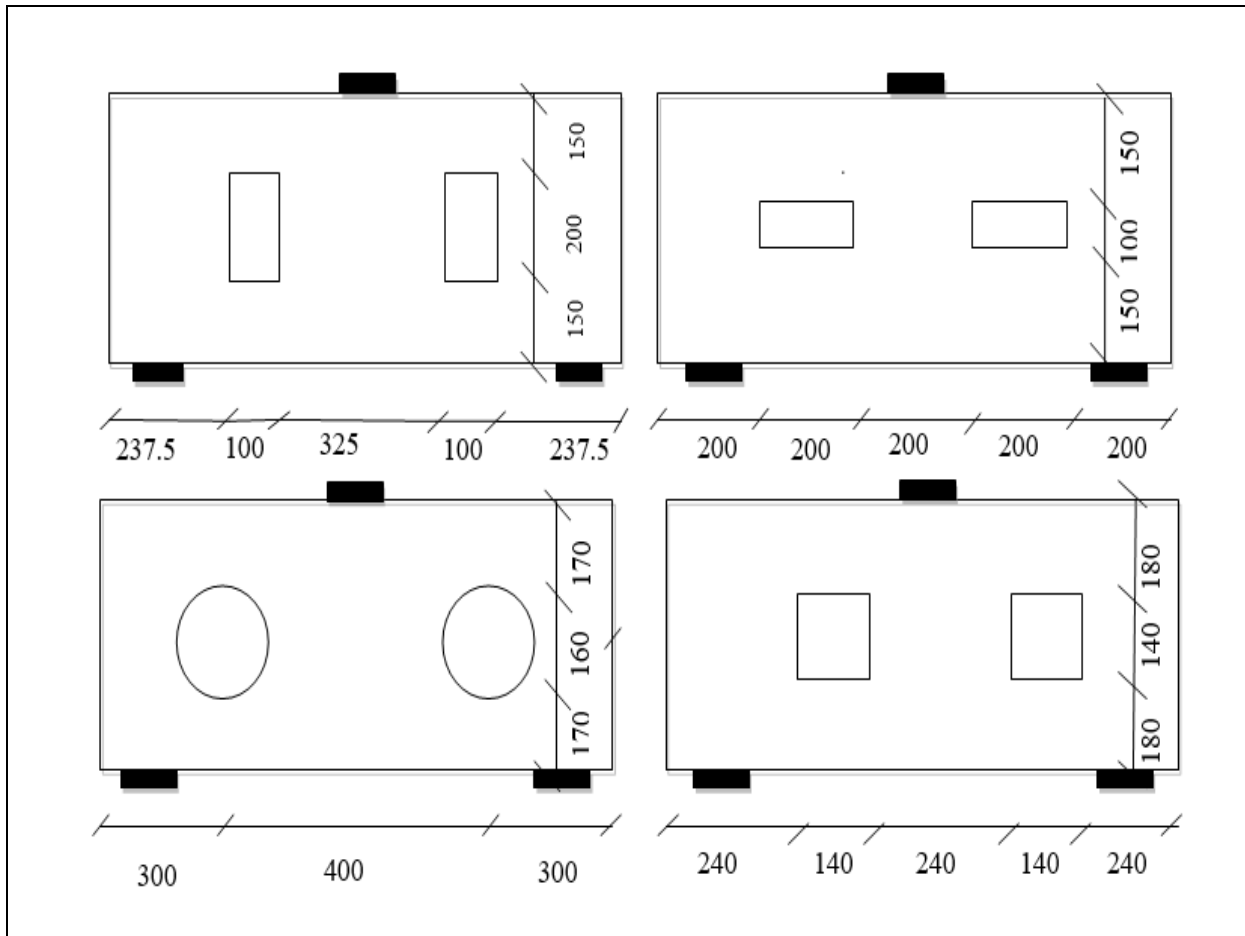


Figure (2) : the locations and dimensions of openings in all specimens

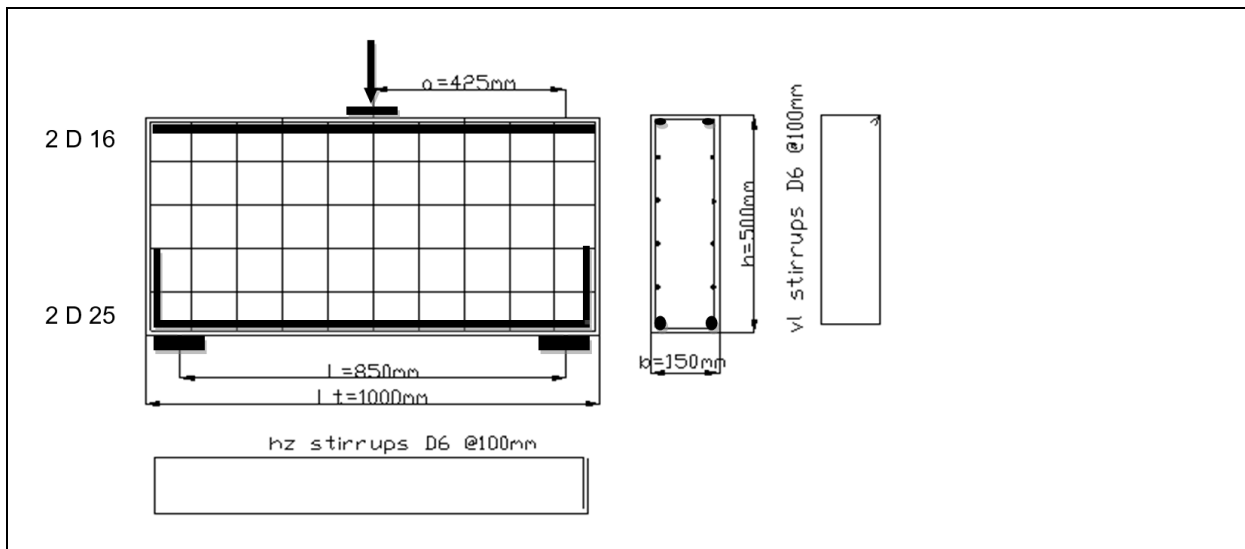


Figure (3): The cross-section and details of reinforcement.

2.3 Test setup

The deep beams are tested at the National Center for Housing and Building Research laboratory. one loading jack is used at the mid-span of the beam. The load cell is attached to a digital screen to record the applying loads and corresponding deflections. The loading system, test setup and the locations of linear variable displacement transducer LVDT are illustrated in Figure (5)

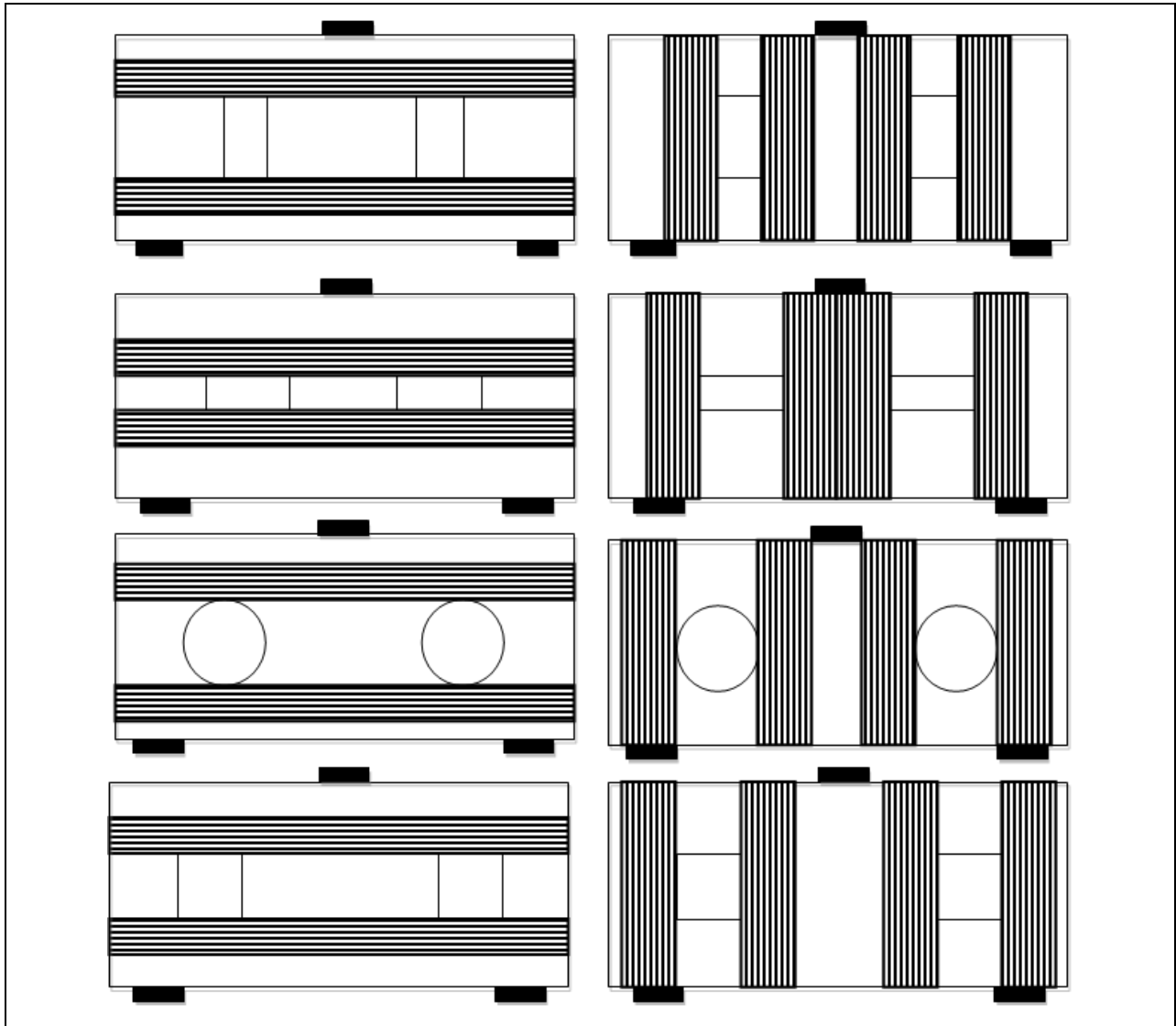


Figure (4): The system of beam strengthening.



Figure (5): The test set-up

3. RESULTS AND DISCUSSION

3.1 Crack pattern

In the control beam (NS-VRO), diagonal fractures started around the apertures and spread to the loading point and supports (figure (6)). In reinforced deep beams with vertical BFRP sheets, the cracking load was roughly 60% of the ultimate load. Deep beams with apertures break later with horizontal reinforcing than vertical reinforcement (Table 3).

In the vertical strengthening in all types of openings, the cracks were confined diagonally between 2 vertical sheets above and below the opening as shown in figure (6), in addition to that they were deep cracks deeper than their counterparts in the horizontal strengthening, and also in the vertical strengthening, no cracks appeared from under the sheets, unlike the horizontal one, in which the cracks appeared under the BFs figure (7). The vertical strengthening hid the inclined cracks that start from the top under the load, while the horizontal reinforcement showed these cracks in all types of openings. The concrete cover in most vertically supported samples was lifted from the bottom or sides during the collapse, while this did not happen in horizontal reinforcement samples

The vertical strengthening using BFRP prevented cracks on both sides of the openings, right and left, changing its path to be under the openings and above, as it divided the deep beam horizontally into two sections of deep beams, one upper and the other lower making two triangles, one above and one below, while the horizontal strengthening did not do that, but rather preserved the same shape as the distribution of cracks in the form of One triangle with the full height of the deep beam, and this is what happened in the horizontal openings

3.2 Modes of failure

The control un-strengthened deep beam failed by forming two separate diagonal fractures in the chords right and left the two apertures, dividing the beam into two halves (Fig. 7). Except for horizontal apertures, failure mechanism did not differ with opening form.

Vertical and horizontal BFRP-strengthened deep beam failure types are demonstrated in Figs. 8 and 9. Two diagonal shear fractures in the opening chords and a concrete cover pull-out caused the reinforced beams to break unexpectedly. Samples reinforced with vertical BFRP sheets failed without tearing or rupturing. When specimen HS-HRO from group [1] failed, the BFRP sheet wrapped horizontally above the entrance ruptured.



Figure (6): crack patten of control deep beam (NS-VRO)



Figure (7): crack patten of deep beam with horizontal openings strengthened with vertical BFRP (VS-HRO)



Figure (8): crack patten of deep beam with horizontal openings strengthened with horizontal BFRP (HS-HRO)

3.3 Load-deflection relationship

Figs. 9–12 illustrate specimen load–deflection curves for groups [1], [2], [3], and [4]. From these figures, we can see that deep beams with vertical, circular, and square openings have the same effect on the load-deflection curve behavior in vertical and horizontal strength, where the curve is linear up to the ultimate load and then decreases nonlinearly until beam failure. However, the ultimate load in horizontal strength is higher than in vertical strengthening (20, 5,14 %) respectively.

Whereas, in the case of the horizontal openings, the behavior of the horizontal strengthening is completely different from the vertical strengthening, as the slope of the line in the horizontal is greater than in the vertical, and also after reaching the maximum load, the behavior remains different in both cases. In the slope of the line or even the maximum load, while in the horizontal BFRP sheets, the maximum load increased by (36%). Hence, Horizontal strength improves the ultimate load in the range of (8-54)% while vertical strength improves the ultimate loads in the range of (0-18)% only (Table 3)

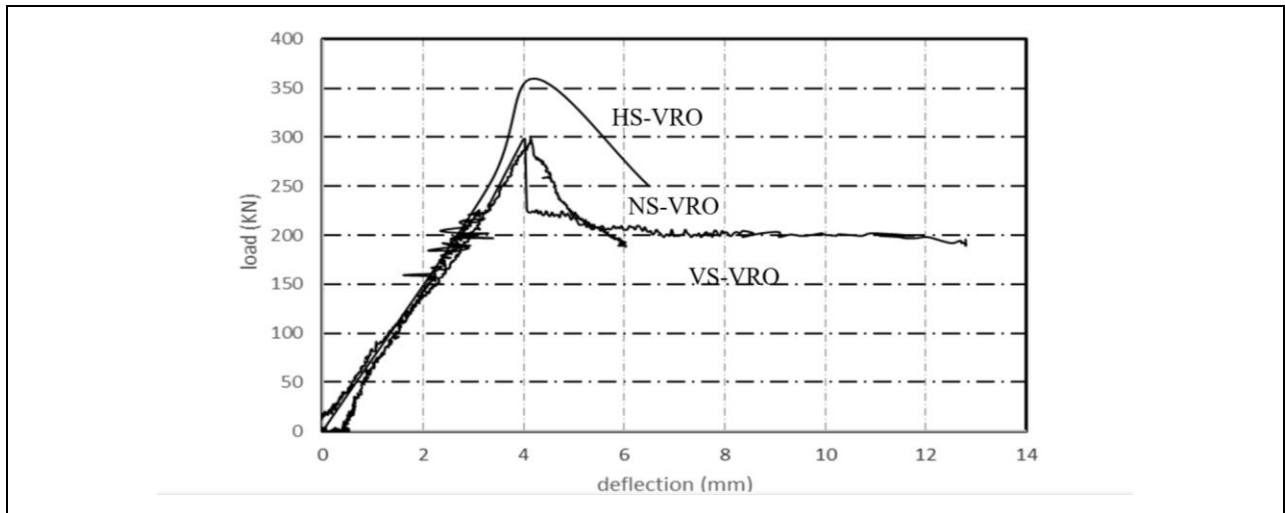


Figure (9): load-deflection curve for group 1

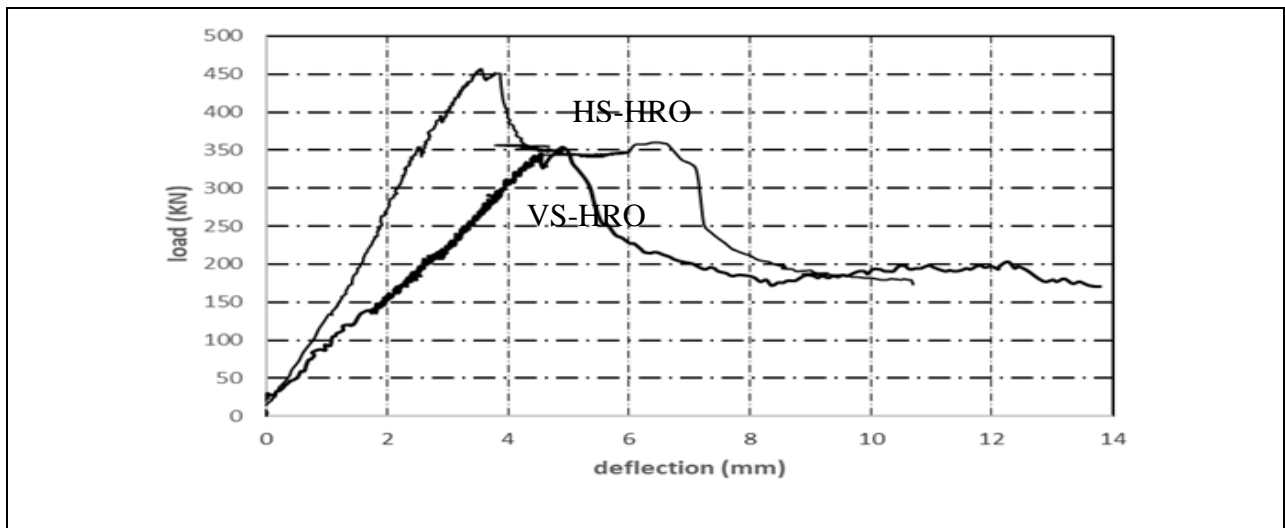


Figure (10): load-deflection curve for group 2

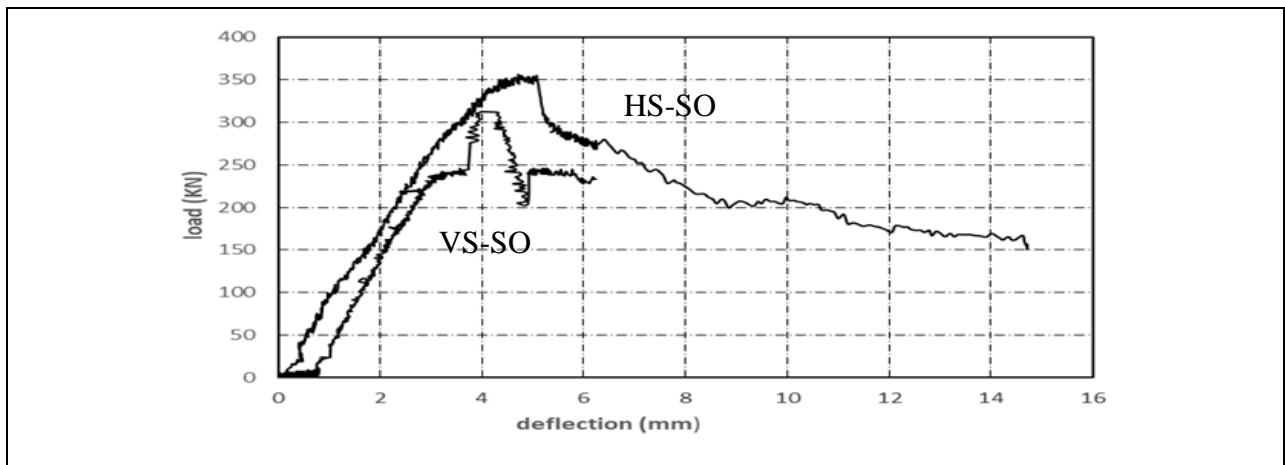


Figure (11): load-deflection curve for group 3

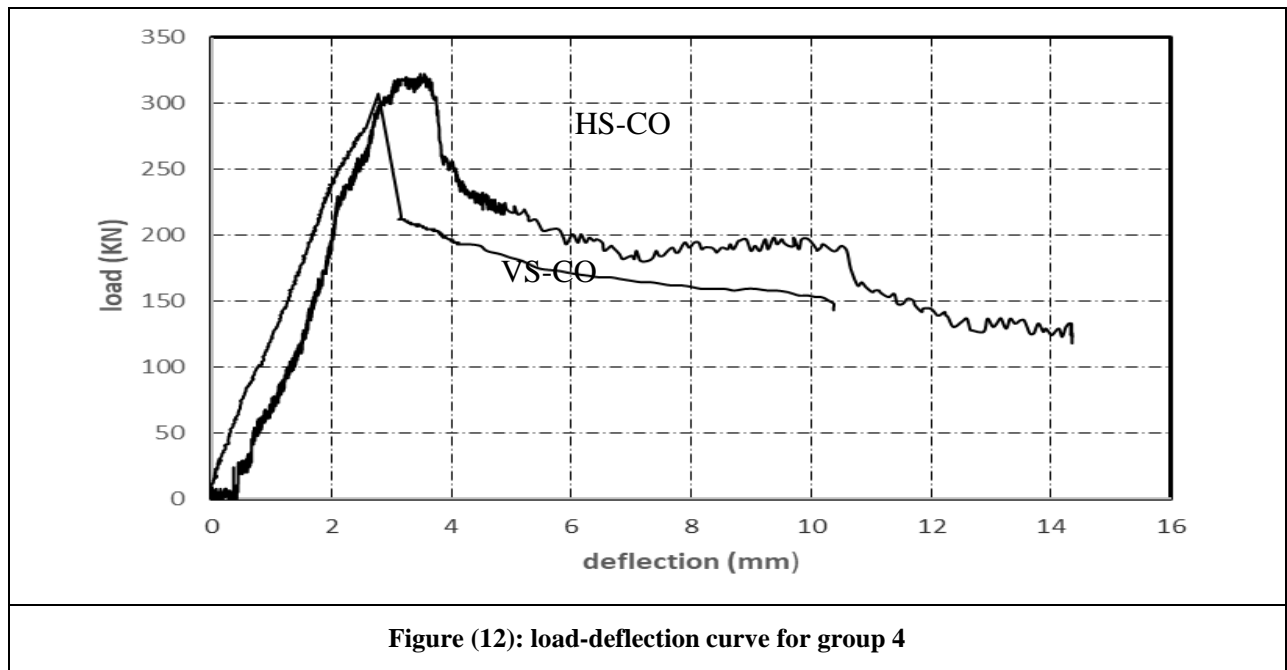


Table 3: The crack loads, ultimate loads values of all beams.

Beam	P cr	P u	(Pcr/pu)%	Improvement in ultimate loads
NS-VRO	178	298.69	59.6	1
VS-VRO	194	298.5	65	1
HS-VRO	250	360	69.44	1.2
VS-HRO	210	353.9	59.3	1.18
HS-HRO	380	456.82	83.2	1.54
VS-CO	181	307.4	58.9	1.03
HS-CO	310	322.53	96.1	1.08
VS-SO	240	312.5	76.8	1.05
HS-SO	325	356.42	91.2	1.19

4. ANALYTICAL MODEL FOR SHEAR STRENGTH PREDICTION

A technique for analysis that predicts the shear strength and accordingly the ultimate load of RC deep beams with openings strengthened with a BFRP sheet is presented in this paper.

$$P_u \text{ expected} = 2(V_f + V_c + V_s) \tag{1}$$

Where V_f = contribution of BFRP sheets to the shear strength. it has been applied using the properties of BFs from testing three specimens of sheets roughed with sand to simulate the contact of basalt and concrete, V_c = contribution of concrete to shear strength, and V_s = contribution of tension steel to shear strength. Equations from (2-12) are listed in The ACI-440 Code, 2014

$$V_f = \frac{A_{vf} * f_{fe} * (\sin \alpha + \cos \alpha) * d_{fv}}{s_f} \tag{2}$$

Where: A_{vf} is the area of sheets fiber (eq.3), f_{fe} is the stress in the fiber sheet which presented in equation (4), α is the angle between the sheet and x-axis, d_{fv} = depth of the FRP sheets and s_f = spacing between strips center from center

$$A_{vf} = 2 * n * t_f * w_f \tag{3}$$

Where t_f = the thickness of the fiber sheets in mm and w_f = width of the sheet in mm

$$f_{fe} = \epsilon_{fe} * E_f \tag{4}$$

Where ϵ_{fe} = strain in the fiber sheets given in eq.5 and E_f = modulus of elasticity of fiber sheets which is calculated from stress -strain curve for 3 tested specimen of BF sheets with roughed surface by sand =5500 MPa

$$\epsilon_{fe} = k_v * \epsilon_{fu} \leq 0.004 \quad (5)$$

Where ϵ_{fu} is the ultimate strain in fiber and we can calculate it using equation (6), K_v is the coefficient of a bond calculated by equation (7)

$$\epsilon_{fu} = \frac{f_{fu}}{E_f} \quad (6)$$

where f_{fu} is the tensile strength of the fiber and E_f = modulus of elasticity for fiber

$$K_v = \frac{k_1 * k_2 * l_e}{11900 \epsilon_{fu}} \quad (7)$$

K_1 and K_2 are factors given in equations (7) and (8), L_e is the bond length of the strip of fiber

$$K_1 = \left(\frac{f'_c}{27}\right)^{2/3} \quad (8)$$

$$K_2 = \frac{d_{fv} - 2l_e}{d_{fv}} \quad \text{for two sides bonded} \quad (9-a)$$

$$K_2 = \frac{d_{fv} - l_e}{d_{fv}} \quad \text{for U-wrapped bonded} \quad (9-b)$$

$$L_e = \frac{23300}{(n_f * t_f * E_f) 0.58} \quad (10)$$

Where n_f is the ratio between modulus of elasticity of concrete E_c and modulus of elasticity of fiber E_f as in equation (11)

$$n_f = E_f / E_c \quad (11)$$

$$\text{and } E_c = 4700 \sqrt{f'_c} \text{ (MPa)} \quad (12)$$

The CIRIA Guide (1977) used Kong and Sharp's (1977) V_c and V_s formula to determine concrete, main, and web steel contributions. Ray, S. P. (1990) streamlined design expression. Equation (13) describes the deep beam with apertures' strength.

$$V_c + V_s = (0.1 f'_c * \lambda_1 * \lambda_2 * \lambda_3 + 0.0085 \psi_s \rho_s f_{sy} + 0.01 \psi_w K_w r_w f_{wy}) x b x D \quad (13)$$

b = beam width, D = beam height, f'_c is the concrete compressive strength.

$$\lambda_1 = \left(1 - \frac{1}{3} \left(\frac{K_1 X_N}{K_2 D}\right)\right) \text{ for } \left(\frac{K_1 X_N}{K_2 D}\right) \leq 1$$

$$= \frac{2}{3} \text{ for } \left(\frac{K_1 X_N}{K_2 D}\right) \geq 1 \quad (14)$$

where $K_1 X_N$ and $K_2 D$ are illustrated in Figure (13)

$$\lambda_2 = (1 - m) \quad (15)$$

Where:

m is the ratio of path length intercepted to total path length along the natural load path =0 for non-interception

$$\lambda_3 = (0.85 \pm 0.3 \left(\frac{e_x}{X_{net}}\right)) (0.85 \pm 0.3 \left(\frac{e_y}{Y_{net}}\right)) \quad (16)$$

where $e_x \leq X_N / 4$, $e_y \leq 0.6D / 4$

$$\text{and } X_{net} = (X_N - a_1 x), Y_{net} = (0.6D - a_2 D) \quad (17)$$

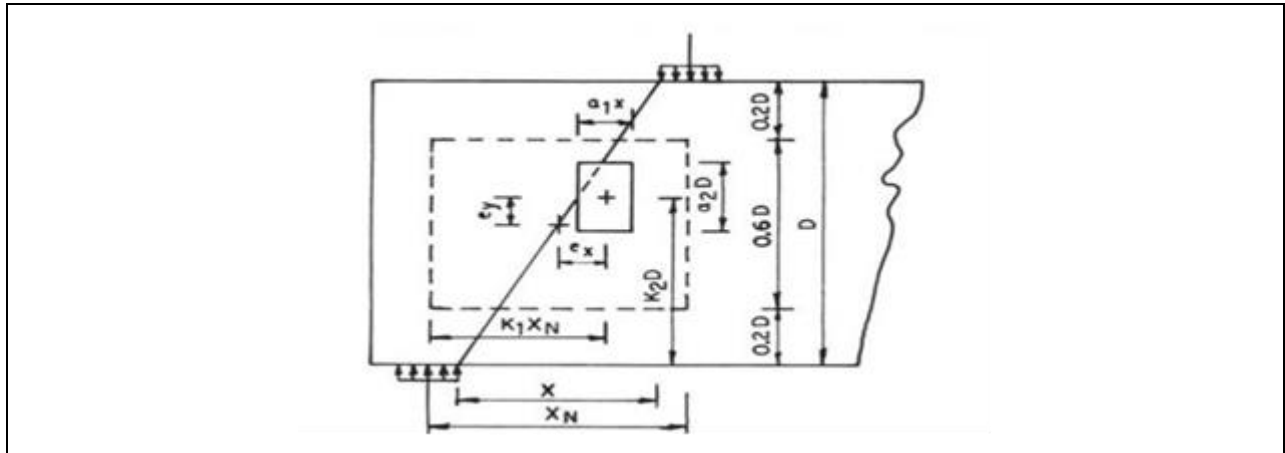


Figure (13): The position of the opening intersects the natural load path

$$\rho_s = A_s / bD * 100\% \quad (16)$$

$$r_w = \sum A_w / bD * 100\% \quad (17)$$

where ψ_s is an empirical coefficient that reflects the levels of stress in main steel = 0.65 and ψ_w is coefficient = 0.50 and $K_w = 0.85$ for Hz bars, $K_w = \cot \beta$ for V1 bars, β is the angle of inclination of the natural load path, F_{sy} is the yield stress of main reinforcement and f_{wy} is the yield stress of web reinforcement.

Table (4) compares analytical and experimental findings. The analytical model is close to the experimental result in reference deep beam (NS-VRO) without BFRP, thus we may estimate the ultimate load for horizontal, circular, and square apertures. The beam (VS-VRO) maximum load did not surpass the analytical model's shear strength. Rotation of three shear span segments caused this beam to collapse prematurely. V-VRO, HRO, CO, SO deep beams reinforced vertically by BFRP. The experimental-to-analytical shear strength ratio was 0.75–0.97 for these specimens. To account for a probable change in failure mode, RC deep beams with vertical BFRP should be strengthened with a strength reduction factor of 0.8. The experimental-to-analytical strength ratio of all horizontally reinforced specimens was 0.7–0.88. This indicates a strength decrease factor of 0.8 for reinforcing RC deep beams with horizontal BFRP to allow for a probable failure mode shift. The analytical model can forecast shear strength for RC deep beams with BFRP-strengthened apertures.

Table (4): Experimental and analytical increase in ultimate load

Beam specimen	Experimental ultimate load P_u (kN)	P_u expected for non-strengthened beam (KN) [1]	V_f (kN) (Ref. 30)	Increase in ultimate load [2]	Total load expected. [1]+ [2]	exp. /expected .
NS-VRO	298.5	300.578	-	-	300.578	0.99
VS-VRO	298.5	300.578	48.3	96.6	397.2	0.75
HS-VRO	360	300.578	71.584	143.168	434.7	0.83
VS-HRO	353.9	299.26	32.2	64.4	363.66	0.97
HS-HRO	456.82	299.26	107.376	214.75	514	0.88
VS-CO	307.4	301.9	37.17	74.34	376.24	0.82
HS-CO	322.53	301.9	82.59	165.18	467.1	0.7
VS-SO	312.5	305.35	40.3	80.6	385.95	0.81
HS-SO	356.42	305.35	89.48	178.96	484.3	0.73

5. CONCLUSION

Based on the experimental and analytical study, the following conclusions can be achieved:

- For deep beams with horizontal web holes, BFRP wrapping may increase shear strengths by up to 54%. The shear strengths of deep beams with web apertures improved by BFRP wrapped vertically can only be increased by 18% with horizontal openings, hence horizontal openings are ideal. Due to deep beams' horizontal shear behavior, circular openings may not be the ideal.
- Horizontal strength of opening is more effective than vertical strength in all types of openings where the horizontal strength improves the ultimate load in the range of (8-54) % while vertical strength improves the ultimate loads only in the range of (0-18) % according to the type of openings
- **In vertical rectangle openings**, the deep beam with horizontal strengthening is higher in ultimate load than that ultimate load in deep beam with vertical strengthening by (20.6%). Also, the cracking load appears later in the deep beam with horizontal strengthening than that in the deep beam with vertical strengthening
- **In horizontal rectangle openings**, the deep beam with horizontal strengthening is higher than the deep beam with vertical strengthening by (29.1%) in ultimate load. Also, the cracking load appears later in the deep beam with horizontal strengthening than that in the deep beam with vertical strengthening, the deflection at ultimate load also is higher in the deep beam with horizontal strength than that in the deep beam with vertical strength.
- **In circle openings**, the horizontal strengthening is higher than the vertical strengthening only by (5%) in ultimate load. Also, the cracking load appears later in the deep beam with horizontal strengthening than that in deep beam with vertical strengthening, the deflection at ultimate load also is higher in deep beam with horizontal strength than that in deep beam with vertical strength.
- **In square openings**, the horizontal strengthening is higher than the vertical strengthening by (14%) in ultimate load. Also, the cracking load appears later in the deep beam with horizontal strengthening than that in the deep beam with vertical strengthening, the deflection at ultimate load also is higher in the deep beam with horizontal strength than that in the deep beam with vertical strength.
- Vertical strength doesn't affect strongly the ultimate load in deep beams with vertical, circular, or square openings
- Kong and Sharp (1977) and Ray, S. P. (1990) empirical formulae may forecast the shear strengths of deep beams with varying apertures and BFRP designs.

REFERENCES

- [1] ACI 440.2R, (2014), Guide for the Design and Construction of Externally Bonded FRP Systems for Strengthening Concrete Structures, American Concrete Institute, Detroit, USA.
- [2] Arabzadeh, A. (2001). Analysis of some experimental results of simply supported deep beams using truss analogy method. *Iranian Journal of Science and Technology. Transaction B, Technology*, **25**(1), 115-128.
- [3] Campione, G., & Minafò, G. (2012). Behaviour of concrete deep beams with openings and low shear span-to-depth ratio. *Engineering Structures*, **41**, 294-306. <https://doi.org/10.1016/j.engstruct.2012.03.055>
- [4] de Paiva, H. R., & Siess, C. P. (1965). Strength and behavior of deep beams in shear. *Journal of the Structural Division*, **91**(5), 19-41. <https://doi.org/10.1061/JSDEAG.0001329>
- [5] El Maaddawy, T., & Sherif, S. (2009). FRP composites for shear strengthening of reinforced concrete deep beams with openings. *Composite Structures*, **89**(1), 60-69. <https://doi.org/10.1016/j.compstruct.2008.06.022>
- [6] El-Kareim, A., Arafa, A., Hassanin, A., Atef, M., & Saber, A. (2020). Behavior and strength of reinforced concrete flanged deep beams with web openings. *Structures*, **27**, 506-524. <https://doi.org/10.1016/j.istruc.2020.06.003>
- [7] Ghali, M. K., Said, M., Mustafa, T. S., & El-Sayed, A. A. (2021). Behaviour of T-shaped RC deep beams with openings under different loading conditions. *Structures*, **31**, 1106-1129. <https://doi.org/10.1016/j.istruc.2021.01.091>
- [8] Guide, C. I. R. I. A. (1977). 2: *The Design of Deep Beams in Reinforced Concrete*. Ove Arup and Partners, Construction Industry Research and Information Association, London.

- [9] Hawileh, R. A., El-Maaddawy, T. A., & Naser, M. Z. (2012). Nonlinear finite element modeling of concrete deep beams with openings strengthened with externally bonded composites. *Materials & Design*, **42**, 378-387. <https://doi.org/10.1016/j.matdes.2012.06.004>
- [10] Hussain, Q., & Pimanmas, A. (2015). Shear strengthening of RC deep beams with openings using sprayed glass fiber reinforced polymer composites (SGFRP): Part 1. Experimental study. *KSCE Journal of Civil Engineering*, **19**, 2121-2133.
- [11] Hwang, S. J., Lu, W. Y., & Lee, H. J. (2000). Shear strength prediction for reinforced concrete corbels. *Structural Journal*, **97**(4), 543-552.
- [12] Karimizadeh, H., & Arabzadeh, A. (2021). A STM-based analytical model for predicting load capacity of deep RC beams with openings. *Structures*, **34**, 1185-1200. <https://doi.org/10.1016/j.istruc.2021.08.052>
- [13] Karimizadeh, H., Arabzadeh, A., Eftekhari, M. R., & Amani Dashlekeh, A. (2022). Shear Strengthening of RC Deep Beams with Symmetrically or Asymmetrically Positioned Square Openings Using CFRP Composites and Steel Protective Frames. *Advances in Civil Engineering*. <https://doi.org/10.1155/2022/5352330>
- [14] Khalaf MR, Al-Ahmed AH, Allawi AA, El-Zohairy A. (2021) Strengthening of continuous reinforced concrete deep beams with large openings using CFRP strips. *Materials*, **14**(11):3119..
- [15] Kong, F. K., & Sharp, G. R. (1977). Structural idealization for deep beams with web openings. *Magazine of Concrete Research*, **29**(99), 81-91. <https://doi.org/10.1680/mac.1977.29.99.81>
- [16] Rahim, N. I., Mohammed, B. S., Al-Fakih, A., Wahab, M. M. A., Liew, M. S., Anwar, A., & Amran, Y. M. (2020). Strengthening the structural behavior of web openings in RC deep beam using CFRP. *Materials*, **13**(12), 2804. <https://doi.org/10.3390/ma13122804>
- [17] Ramakrishnan, V., & Ananthanarayana, Y. (1968). Ultimate strength of deep beams in shear. In *Journal Proceedings*, **65**(2), 87-98. <https://doi.org/10.14359/7458>
- [18] Ramakrishnan, V., & Panchalan, R. K. (2005). A new construction Material—Non-corrosive basalt bar reinforced concrete. *Special Publication*, **229**, 253-270. <https://doi.org/10.14359/14741>
- [19] Ray, S. P. (1990). Deep beams with web openings. *Reinforced concrete deep beams*, 288.
- [20] Shetty, M. S., & Jain, A. K. (2019). *Concrete Technology (Theory and Practice)*, 8e. S. Chand Publishing.
- [21] WY Lu, HW Yu, CL Chen, SL Liu(2015) "High-strength concrete deep beams with web openings strengthened by carbon fiber reinforced plastics." *Computers and Concrete*.